

Exact spectral functions of a non-Fermi liquid in one dimension

Karlo Penc¹ and B. Sriram Shastry²

¹Research Institute for Solid State Physics and Optics, P.O. Box 49, H-1525 Budapest, Hungary

²Bell Laboratories, Lucent Technologies, Murray Hill, New Jersey 07974

and Indian Institute of Science, Bangalore 560012, India

(Received 18 September 2001; revised manuscript received 11 January 2002; published 29 March 2002)

We study the exact one-electron propagator and spectral function of a solvable model of interacting electrons due to Schulz and Shastry. The solution previously found for the energies and wave functions is extended to give spectral functions that turn out to be computable, interesting, and nontrivial. They provide one of the few examples of cases where the spectral functions are known asymptotically as well as exactly.

DOI: 10.1103/PhysRevB.65.155110

PACS number(s): 71.27.+a, 79.60.-i

I. INTRODUCTION

The excitations of a one-dimensional (1D) interacting Fermi system cannot be explained using quasiparticles of the Fermi-liquid picture. For example, the momentum distribution function has a cusp at the Fermi momentum k_F rather than a jump as in a Fermi liquid.^{1,2} This behavior is of the kind first found by Luttinger in the context of his study of an exactly solvable one-dimensional model.³ The fermionic Green's functions are nontrivial, and the asymptotic long-distance behavior has characteristic singularities that are popularly known as the Tomonaga-Luttinger liquid behavior.^{4,5} On the other hand, very little is known beyond the asymptotic or low-energy regime. A few exact analytical calculations of the spectral function for model systems are available in literature, and they are all in the strongly correlated limit, where the double occupancy of a site is projected out: this includes the Hubbard model in the limit of infinitely large repulsion^{6,7} and the $1/r^2$ exchange t - J model.^{8,9}

Recently Schulz and Shastry¹⁰ introduced a new class of gauge coupled 1D Fermi systems, which make it possible to study the behavior of the spectral function starting from a weakly interacting limit. These models are similar in nature to those of Ref. 11, and are non-Fermi liquids due to the gauge coupling. Details of the various inter-relationships are reviewed in Ref. 12. The model introduced by Schulz and Shastry (SS) is in fact intimately connected to the original Luttinger model, and is best viewed as its reinterpretation as a gauge theory. Particles of different species exert a mutual gauge potential on each other and this is sufficient to destroy the Fermi liquid. The asymptotic long-distance behavior of the one-electron correlation function is known (see below) by one of several arguments, including Luttinger's original one using the asymptotic properties of Toeplitz determinants.

Our motivation in the present work is to compute the exact one-electron Green's function for the SS model, utilizing our knowledge of the complete spectrum of the same, and using techniques familiar from Anderson's treatment of the orthogonality catastrophe issue in the x-ray edge problem.¹³ This is of great interest since usually one does not have access to the exact Green's function even in 1D and one has to be content with the asymptotic behavior. For interpreting experiments, such as those on photoemission, one wants to know more than just the asymptotics, and this possibility

is realized here for the particular model of SS. We are able to see how the Luttinger-liquid spectral function evolves from a noninteracting free fermion case by switching on some interaction parameter.

We first write down the basic lattice Fermi model in 1D and outline the pseudounitary transformation that eliminates the gauge interactions in favor of a twisted boundary condition (Sec. II). Using this transformation we formulate the problem of calculating the one-electron Green's function in Sec. III.

II. THE MODEL

Let us write the model for two-component electrons hopping and interacting via the Hamiltonian

$$\mathcal{H} = -t \sum_{j=0}^{L-1} \sum_{\sigma} \exp(i\sigma\alpha[\hat{n}_{j,\bar{\sigma}} + \hat{n}_{j+1,\bar{\sigma}}]) c_{j,\sigma}^{\dagger} c_{j+1,\sigma} + \text{H.c.}, \quad (1)$$

where for concreteness we have simplified the original model presented in Ref. 10. Here L denotes the number of sites in the chain, $c_{j,\sigma}^{\dagger}$ creates a fermion with spin $\sigma = \uparrow, \downarrow$ at site j , $\hat{n}_{j,\bar{\sigma}} = c_{j,\bar{\sigma}}^{\dagger} c_{j,\bar{\sigma}}$ is the occupation operator with $\bar{\sigma} = -\sigma$, and by N_{σ} we will denote the total number of σ spin fermions, which is the eigenvalue of the operator \hat{N}_{σ} . Finally, t is the hopping parameter and the gauge interaction is controlled by the dimensionless parameter in our model, α . The unitary transformation

$$\mathcal{U}_1 = \exp\left(i \sum_{l>m} \alpha[\hat{n}_{l,\uparrow} \hat{n}_{m,\downarrow} - \hat{n}_{m,\uparrow} \hat{n}_{l,\downarrow}]\right) \quad (2)$$

transforms Eq. (1) into a simple hopping Hamiltonian with twisted boundary conditions.¹⁰ To regain a translational invariant Hamiltonian we apply a second unitary transformation

$$\mathcal{U}_2 = \prod_{l=0}^{L-1} \exp\left(\frac{2i\alpha l(\hat{N}_{\uparrow} \hat{n}_{l,\downarrow} - \hat{N}_{\downarrow} \hat{n}_{l,\uparrow})}{L}\right). \quad (3)$$

The combined transformation $\mathcal{U}=\mathcal{U}_2\mathcal{U}_1$ commutes with \mathcal{T} , where \mathcal{T} is the translational operator that shifts one site to the right (e.g., $\mathcal{T}\hat{n}_j\mathcal{T}^\dagger=\hat{n}_{j+1}$). The effect of \mathcal{U} on the fermion operators is

$$\begin{aligned} \mathcal{U}c_{j,\sigma}^\dagger\mathcal{U}^\dagger &= e^{-i\alpha\sigma N_{\bar{\sigma}}}e^{i\alpha\sigma\hat{n}_{j,\bar{\sigma}}}c_{j,\sigma}^\dagger \\ &\times \prod_{l=0}^{j-1} \exp(2i\alpha\sigma\hat{n}_{l,\bar{\sigma}}) \prod_{l=0}^{L-1} \exp\left(\frac{2i\sigma(l-j)\alpha\hat{n}_{l,\bar{\sigma}}}{L}\right), \\ \mathcal{U}c_{j,\sigma}\mathcal{U}^\dagger &= e^{i\alpha\sigma N_{\bar{\sigma}}}e^{-i\alpha\sigma\hat{n}_{j,\bar{\sigma}}}c_{j,\sigma} \\ &\times \prod_{l=0}^{j-1} \exp(-2i\alpha\sigma\hat{n}_{l,\bar{\sigma}}) \prod_{l=0}^{L-1} \\ &\times \exp\left(\frac{-2i\sigma(l-j)\alpha\hat{n}_{l,\bar{\sigma}}}{L}\right), \end{aligned} \quad (4)$$

while the density operators, $\mathcal{U}\hat{n}_{j,\sigma}\mathcal{U}^\dagger=\hat{n}_{j,\sigma}$, as well as the S_j^z spin operator are invariant (the S_j^+ and S_j^- spin operators are not invariant under the transformation). The transformed Hamiltonian $\tilde{\mathcal{H}}=\mathcal{U}\mathcal{H}\mathcal{U}^\dagger$ reads

$$\tilde{\mathcal{H}}=-t\sum_{j=0}^{L-1}\sum_{\sigma} (e^{2i\sigma\alpha n_{\bar{\sigma}}}c_{j,\sigma}^\dagger c_{j+1,\sigma}+\text{H.c.}), \quad (5)$$

where $n_{\sigma}=\hat{N}_{\sigma}/L$ is the density operator of σ spin fermions. In a fixed number subspace, we may treat n_{σ} as a ‘‘c number.’’ Thus we see that the transformed hopping has a ‘‘dynamically generated’’ gauge field. In the eigenvalue problem

$$\tilde{\mathcal{H}}|\tilde{\phi}\rangle=E|\tilde{\phi}\rangle; \quad (6)$$

the eigenstates $|\tilde{\phi}\rangle$ are products of noninteracting one-particle states with momenta k created with $c_{k,\sigma}^\dagger=L^{-1/2}\sum_l e^{ikl}c_{l,\sigma}^\dagger$ operator, $|\tilde{\phi}\rangle=\prod_{k,\sigma}c_{k,\sigma}^\dagger|0\rangle$. The momenta are quantized as $Lk_{j,\sigma}=2\pi\mathcal{I}_{j,\sigma}$, $\mathcal{I}_{j,\sigma}$ being an integer. The total energy and momentum of the states is

$$E=\sum_{\sigma}\sum_{j=1}^{N_{\sigma}}\varepsilon_{\sigma}(k_{j,\sigma}), \quad P=\sum_{\sigma}\sum_{j=1}^{N_{\sigma}}k_{j,\sigma}, \quad (7)$$

and the one-particle energy is

$$\varepsilon_{\sigma}(k)=-2t\cos(k+2\sigma\alpha n_{\bar{\sigma}}). \quad (8)$$

Thus we must have the eigenstates of \mathcal{H} ,

$$|\phi\rangle=U^\dagger|\tilde{\phi}\rangle, \quad (9)$$

with the energy and momentum given also by Eq. (7). In the ground state the k states between the Fermi momenta $k_{F,\sigma}^-$ and $k_{F,\sigma}^+$ are filled ($k_{F,\sigma}^\pm=\pm\pi n_{\sigma}-2\alpha\sigma n_{\bar{\sigma}}$). In the thermodynamic limit the energy E does not depend on α and is equal to the energy of the noninteracting $\alpha=0$ case. For finite-size systems α enters only through the $O(1/L)$ corrections.

For general α the Hamiltonian breaks both the parity (P) and time inversion (T) symmetry (the combined PT symme-

try is conserved). In the ground state the gauge interaction act like a vector potential and generates currents that flow in the opposite directions for opposite spins. As a consequence the Fermi momenta are also shifted. For the $\alpha=\pm\pi$ case both P and T are restored and the Fermi momenta again coincide for the two spin directions.

III. SPECTRAL FUNCTIONS

Our goal is to calculate the spectral functions, which we define as

$$A_{\sigma}(k,\omega)=\sum_f | \langle f|c_{k,\sigma}^\dagger|G\rangle|^2 \delta(\omega-E_f^{N+1}+E_{\text{GS}}), \quad (10)$$

$$B_{\sigma}(k,\omega)=\sum_f | \langle f|c_{k,\sigma}|G\rangle|^2 \delta(\omega-E_{\text{GS}}+E_f^{N-1}), \quad (11)$$

where $|G\rangle$ denotes the ground state. The local (k averaged) spectral functions are defined as

$$A_{\sigma}(\omega)=\frac{1}{L}\sum_k A_{\sigma}(k,\omega), \quad (12)$$

$$B_{\sigma}(\omega)=\frac{1}{L}\sum_k B_{\sigma}(k,\omega). \quad (13)$$

We concentrate on $A_{\uparrow}(k,\omega)$, since $B_{\sigma}(k,\omega)$ is calculated analogously.

As mentioned in the Introduction, 1D interacting fermions behave as Tomonaga-Luttinger liquids, which are characterized, among others, by the power-law behavior of the correlation function for small energies. In our case, as we will see later, the main contribution for $0<\alpha<\pi$ comes from

$$\begin{aligned} A_{\uparrow}(k,\omega) \approx c_1 &\frac{[(\omega-\varepsilon_F)^2-u^2(k-k_{\uparrow}^{(-)})^2]^{(\alpha/\pi)^2}}{\omega-\varepsilon_F-u(k-k_{\uparrow}^{(-)})} \\ &+ c_1 \frac{[(\omega-\varepsilon_F)^2-u^2(k-k_{\uparrow}^{(1)})^2]^{(\alpha/\pi)^2}}{\omega-\varepsilon_F+u(k-k_{\uparrow}^{(1)})} \\ &+ c_2 \frac{[(\omega-\varepsilon_F)^2-u^2(k-k_{\uparrow}^{(1)})^2]^{(\alpha/\pi-1)^2}}{\omega-\varepsilon_F-u(k-k_{\uparrow}^{(1)})} \\ &+ c_2 \frac{[(\omega-\varepsilon_F)^2-u^2(k-k_{\uparrow}^{(3)})^2]^{(\alpha/\pi-1)^2}}{\omega-\varepsilon_F+u(k-k_{\uparrow}^{(3)})}, \end{aligned} \quad (14)$$

where $k_{\sigma}^{(\nu)}=\nu\pi n_{\sigma}-2\sigma\alpha n_{-\sigma}$ are the (Fermi) momenta of the singularities, c_1 and c_2 are constants, and u is the velocity of the excitations. In the usual Tomonaga-Luttinger liquids the velocities of the spin and charge excitations are different and they both appear in spectral functions. In our case, however, due to the gauge origin of the interaction, the spin and charge velocities are equal to the Fermi velocity v_F . The spectral function has a nonanalytical, branch cut structure not only at the Fermi momenta, but for a higher multiple of the Fermi momenta ($k_{\uparrow}^{(3)}$) as well. The latter corresponds, e.g.,

to the $3k_F$ singularity, e.g., in the Hubbard model,^{2,7} but unlike in that case, has an exponent that is as large as that of the Fermi point $k_{\uparrow}^{(1)}$. The local density of states near Fermi energy reads

$$A(\omega) \approx c_1(\omega - \varepsilon_F)^{2(\alpha/\pi)^2} + c_2(\omega - \varepsilon_F)^{2(\alpha/\pi - 1)^2}, \quad (15)$$

which for the noninteracting $\alpha=0$ reproduces the Fermi-liquid step function.

The exponent were already obtained from the finite-size analysis of the energy, with $\delta=2\alpha$ in Eq. (9) of Ref. 10. Before continuing, let us mention that while we have all the typical features of a Tomonaga-Luttinger model (the algebraic singularities and low-lying excitations at multiples of the Fermi momenta), the strong asymmetry of the spectra due to the gauge interaction is not a typical feature of the standard Luttinger liquids.

We now consider the exact evaluation of the spectral functions. As a preliminary to the discussion for general α , let us note the special cases of $\alpha=0$ and $\alpha=\pi$, where the spectral functions can be calculated more or less trivially.

(i) The $\alpha=0$ case is nothing else but the usual tight-binding Hamiltonian

$$\mathcal{H} = -t \sum_{j,\sigma} (c_{j,\sigma}^\dagger c_{j+1,\sigma} + \text{H.c.}) \quad (16)$$

of noninteracting electrons, as $e^{i\alpha n_j} = 1$ in Eq. (1). For the spectral functions we recover the familiar

$$A_\sigma^{(0)}(k, \omega) = \delta(\omega + 2t \cos k) \Theta(\omega - \varepsilon_F), \quad (17)$$

$$B_\sigma^{(0)}(k, \omega) = \delta(\omega + 2t \cos k) \Theta(\varepsilon_F - \omega), \quad (18)$$

i.e., a Dirac-delta peak following the cosinelike dispersion of the free fermions.

(ii) When $\alpha=\pi$, the model actually corresponds to the electron-hole symmetric correlated hopping model¹⁴ with $t_{AA} = t_{BB} = -t$ and $t_{AB} = t$ (the hopping amplitudes t_{AA} , t_{BB} , and t_{AB} are defined in Ref. 14),

$$\mathcal{H} = -t \sum_{j,\sigma} (1 - 2\hat{n}_{j,\bar{\sigma}})(1 - 2\hat{n}_{j+1,\bar{\sigma}})c_{j,\sigma}^\dagger c_{j+1,\sigma} + \text{H.c.} \quad (19)$$

The Hamiltonian (19) can be diagonalized with the help of a unitary transformation

$$\tilde{U} = \prod_{j=1}^L (-1)^{\hat{n}_{j,\uparrow}\hat{n}_{j,\downarrow}}, \quad (20)$$

which is simpler than $\tilde{U} = \tilde{U}_1 \tilde{U}_2$ given by Eqs. (2) and (3), and transforms the fermionic operators as

$$\tilde{U} c_{j,\sigma}^\dagger \tilde{U}^\dagger = (1 - 2\hat{n}_{j,\bar{\sigma}}) c_{j,\sigma}^\dagger,$$

$$\tilde{U} c_{j,\sigma} \tilde{U}^\dagger = (1 - 2\hat{n}_{j,\bar{\sigma}}) c_{j,\sigma}, \quad (21)$$

so the transformed fermionic operators remain ‘‘local.’’ Furthermore, this transformation is not any more restricted to the 1D case. The evaluation of the matrix elements is now

convenient for operators in site representation, and the matrix element in Eq. (10) becomes

$$|\langle f | c_{k,\uparrow}^\dagger | G \rangle|^2 = L |\langle f | c_{0,\uparrow}^\dagger | G \rangle|^2 \delta_{k, P_f - P_{GS}}, \quad (22)$$

where $c_{0,\uparrow}^\dagger$ creates fermions at site 0. Next, we apply the canonical transformation to formulate the problem using the transformed wave function [the analog of Eq. (9)], and for the spectral function we get

$$A_\uparrow(k, \omega) = L \sum_{\tilde{f}} |\langle \tilde{f} | (1 - 2\hat{n}_{j,\downarrow}) c_{j,\uparrow}^\dagger | \tilde{G} \rangle|^2 \times \delta(\omega - E_f^{N+1} + E_{GS}) \delta_{k, P_f^{N+1} - P_{GS}}.$$

As the wave functions $|\tilde{f}\rangle$ and $|\tilde{G}\rangle$ are products of the spin-up and spin-down part, the evaluation is straightforward and leads to

$$A_\uparrow(k, \omega) = (1 - 2n_\downarrow)^2 A_\uparrow^{(0)}(k, \omega) + \frac{4}{L^2} \sum_{q \in \text{FS}_\downarrow} \sum_{q' \notin \text{FS}_\downarrow} \sum_{k' \notin \text{FS}_\uparrow} \delta(\omega - \varepsilon_\downarrow(q') + \varepsilon_\downarrow(q) - \varepsilon_\uparrow(k')) \delta_{k, q' - q + k'}, \quad (23)$$

and a similar equation gives $B_\uparrow(k, \omega)$. In the spectral function we can identify the following two distinct features: (a) a Dirac-delta contribution following the cosinelike dispersion, which is the reminder of the noninteracting spectral function [Eq. (17)] suppressed by a factor of $(1 - 2n_\downarrow)^2$ and (b) a broader continuum coming from the propagator dressed with a single loop. As we increase the filling, the weight of the Fermi jump for zero magnetization ($n_\uparrow = n_\downarrow = n/2$) decreases as $(1 - n)^2$ and will disappear at half-filling, leaving us with an $A(\omega) \propto \omega^2$ density of states [$c_2 \sim (1 - n)^2$ in Eq. (15) for $\alpha = \pi$]. To illustrate this behavior, we present the evolution of the local spectral functions with density in Fig. 1.

Let us now consider the nontrivial generic case $0 < \alpha < \pi$. Like in the previous case, in evaluating the matrix elements we exploit the translation invariance to derive the site representation given by Eq. (22). Next, we apply the canonical transformation to formulate the problem using the transformed wave functions

$$\langle f | c_{0,\uparrow}^\dagger | G \rangle = \langle \tilde{f} | c_{0,\uparrow}^\dagger e^{i\alpha \hat{n}_{0,\downarrow}} \hat{R} | \tilde{G} \rangle e^{-i\alpha N_\downarrow}, \quad (24)$$

where the important global operator [see Eq. (4)]

$$\hat{R} = \prod_l \exp(2i\alpha l \hat{n}_{l,\downarrow} / L). \quad (25)$$

As in the transformed basis the wave functions are products of the spin-up and -down free fermion wave functions, $|\tilde{G}\rangle = |\tilde{G}_\uparrow\rangle |\tilde{G}_\downarrow\rangle$ and $|\tilde{f}\rangle = |\tilde{f}_\uparrow\rangle |\tilde{f}_\downarrow\rangle$, the matrix element factorizes, and we get

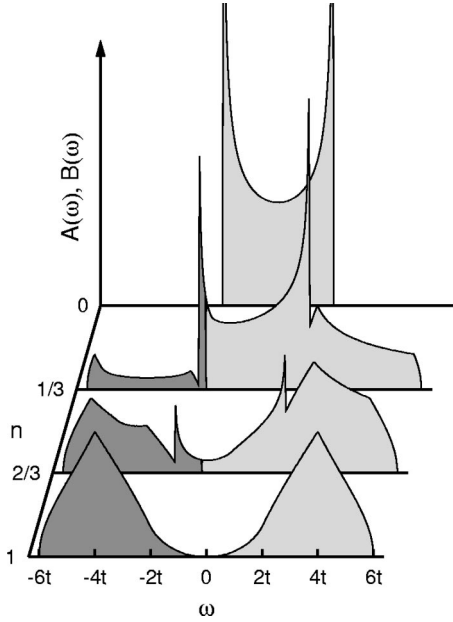


FIG. 1. The local spectral functions $B(\omega)$ (darker) and $A(\omega)$ (lighter shading) for $\alpha = \pi$. The filling increases from $n=0$ (top curve) to $n=1$ (bottom plot) in increments of $1/3$.

$$A_{\uparrow}(k, \omega) = L \sum_{\tilde{f}} |\langle \tilde{f}_{\uparrow} | c_{0,\uparrow}^{\dagger} | \tilde{G}_{\uparrow} \rangle|^2 |\langle \tilde{f}_{\downarrow} | e^{i\alpha \hat{n}_{0,\downarrow}} \hat{R} | \tilde{G}_{\downarrow} \rangle|^2 \\ \times \delta(\omega - E_{f,\uparrow} + E_{GS,\uparrow} - E_{f,\downarrow} + E_{GS,\downarrow}) \\ \times \delta_{k, P_{f,\uparrow} - P_{GS,\uparrow} + P_{f,\downarrow} - P_{GS,\downarrow}}.$$

In the equation above $c_{0,\uparrow}^{\dagger}$ creates a fermion with energy $\varepsilon_{\uparrow}(k')$ and momentum $k' \notin \text{FS}_{\uparrow}$, in which case the matrix element is $|\langle \tilde{f}_{\uparrow} | c_{0,\uparrow}^{\dagger} | \tilde{G}_{\uparrow} \rangle|^2 = 1/L$. This allows us to write the spectral function as a convolution

$$A_{\uparrow}(k, \omega) = \frac{1}{L} \sum_{k' \notin \text{FS}_{\uparrow}} A'_{\uparrow}(k - k', \omega - \varepsilon_{\uparrow}(k')) \quad (26)$$

with

$$A'_{\uparrow}(\omega, k) = L \sum_{\tilde{f}_{\downarrow}} |\langle \tilde{f}_{\downarrow} | e^{i\alpha \hat{n}_{0,\downarrow}} \hat{R} | \tilde{G}_{\downarrow} \rangle|^2 \delta(\omega - E_{f,\downarrow} \\ + E_{GS,\downarrow}) \delta_{k, P_{f,\downarrow} - P_{GS,\downarrow}}. \quad (27)$$

The interesting and nontrivial part of the calculation comes from the $\langle \tilde{f}_{\downarrow} | e^{i\alpha \hat{n}_{0,\downarrow}} \hat{R} | \tilde{G}_{\downarrow} \rangle$ matrix element. In the next and crucial step, we eliminate $e^{i\alpha \hat{n}_{0,\downarrow}}$. This can be easily accomplished after the observation that by translating the operator \hat{R} a similar factor appears: $\mathcal{T} \hat{R} \mathcal{T}^{\dagger} = \exp[2i\alpha(\hat{n}_{0,\downarrow} - n_{\downarrow})] \hat{R}$. So

$$\langle \tilde{f}_{\downarrow} | e^{2i\alpha \hat{n}_{0,\downarrow}} \hat{R} | \tilde{G}_{\downarrow} \rangle = \exp[i(2\alpha n_{\downarrow} - P_{f,\downarrow} + P_{GS,\downarrow})] \langle \tilde{f}_{\downarrow} | \hat{R} | \tilde{G}_{\downarrow} \rangle. \quad (28)$$

Next, we note that $e^{i\alpha \hat{n}_{0,\downarrow}} = (e^{i\alpha} + e^{i2\alpha \hat{n}_{0,\downarrow}}) / (1 + e^{i\alpha})$ and we end up with the useful identity

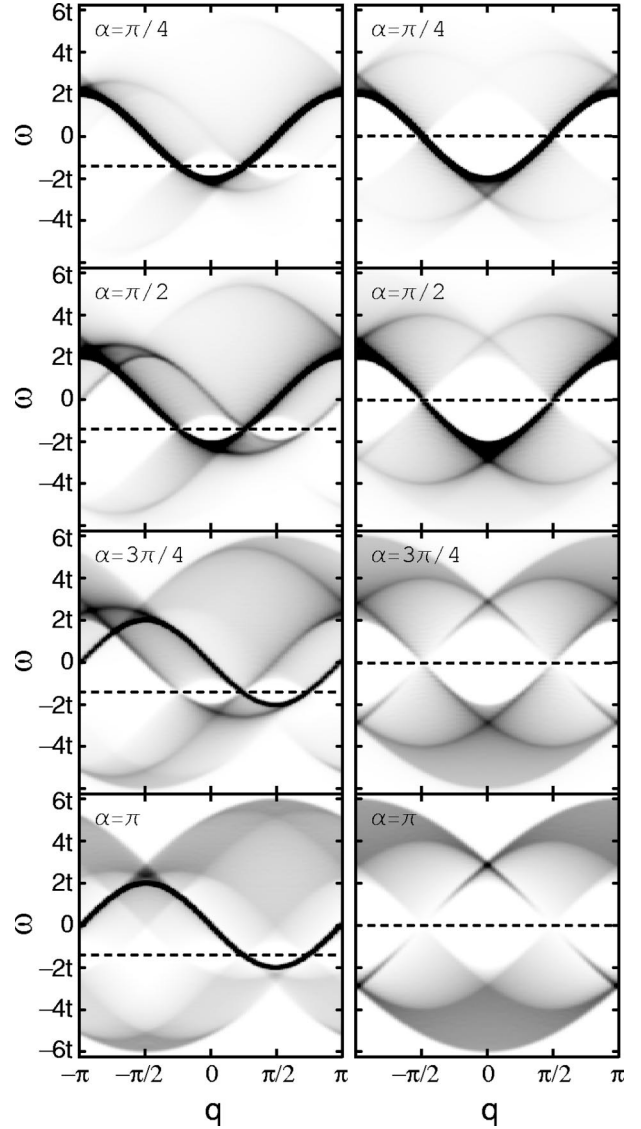


FIG. 2. The evolution of the ω and k dependent spectral function as a function of α for $n=1/2$ (left) and $n=1$ (right plots). The shading is proportional to $A_{\uparrow}(k, \omega)$ and $B_{\uparrow}(k, \omega)$, the dashed line denotes the Fermi energy. The shift of the Fermi momenta [Eq. (35)] is compensated for by introducing $q = k + \alpha n$ in the plot. We omitted the trivial $\alpha=0$ case.

$$\langle \tilde{f}_{\downarrow} | e^{i\alpha \hat{n}_{0,\downarrow}} \hat{R} | \tilde{G}_{\downarrow} \rangle \\ = \frac{e^{i\alpha} + \exp[i(P_{GS,\downarrow} - P_{f,\downarrow} + 2\alpha n_{\downarrow})]}{1 + e^{i\alpha}} \langle \tilde{f}_{\downarrow} | \hat{R} | \tilde{G}_{\downarrow} \rangle. \quad (29)$$

To evaluate $\langle \tilde{f}_{\downarrow} | \hat{R} | \tilde{G}_{\downarrow} \rangle$, we put $|\tilde{G}_{\downarrow}\rangle = \Pi_j c_{k_j,\downarrow}^{\dagger} |0\rangle$ and $|\tilde{f}_{\downarrow}\rangle = \Pi_i c_{k'_i,\downarrow}^{\dagger} |0\rangle$. Then we move \hat{R} to the right across c_k^{\dagger} 's so that it acts on the vacuum state, $\hat{R}|0\rangle = |0\rangle$. However, as $\hat{R} c_{k,\downarrow}^{\dagger} = c_{k+(2\alpha/L),\downarrow}^{\dagger} \hat{R}$, the k momenta are shifted by $2\alpha/L$ (this is equivalent to twisting the boundary conditions),

$$\begin{aligned} \langle \tilde{f}_\downarrow | \hat{R} | \tilde{G}_\downarrow \rangle &= \langle 0 | \prod_{i=1}^{N_\downarrow} c_{k'_i, \downarrow} \hat{R} \prod_{j=1}^{N_\downarrow} c_{k_j, \downarrow}^\dagger | 0 \rangle \\ &= \langle 0 | \prod_{i=1}^{N_\downarrow} c_{k'_i, \downarrow} \prod_{j=1}^{N_\downarrow} c_{k_j + 2\alpha/L, \downarrow}^\dagger | 0 \rangle. \end{aligned} \quad (30)$$

Here we have to calculate overlap of free fermion wave functions with different phase shifts due to the removal of a \uparrow -spin fermion. This very problem arises, e.g., in the x-ray edge problem (the Anderson orthogonality catastrophe¹³), and the one-dimensional analog was discussed in Ref. 7. For the reader's convenience, we repeat here the main points.

The anticommutation relation between the operators with different phase shifts reads

$$\begin{aligned} A_{ij} &= \{c_{k_i + 2\alpha/L, \downarrow}^\dagger, c_{k'_j, \downarrow}\} \\ &= \frac{e^{i\alpha} \exp\left[\frac{i}{2}\left(k_i - k'_j + \frac{2\alpha}{L}\right)\right]}{L} \frac{\sin \alpha}{\sin\left(\frac{k_i - k'_j}{2} + \frac{\alpha}{L}\right)}. \end{aligned} \quad (31)$$

The overlap of the wave functions can be further calculated as $|\langle \tilde{f}_\downarrow | \hat{R} | \tilde{G}_\downarrow \rangle|^2 = |\det A_{ij}|^2$,

$$\begin{aligned} |\langle \tilde{f}_\downarrow | \hat{R} | \tilde{G}_\downarrow \rangle|^2 &= \left\| \begin{array}{ccc} \{c_{k_1 + 2\alpha/L, \downarrow}^\dagger, c_{k'_1, \downarrow}\} & \dots & \{c_{k_1 + 2\alpha/L, \downarrow}^\dagger, c_{k'_{N_\downarrow}, \downarrow}\} \\ \vdots & \ddots & \vdots \\ \{c_{k_{N_\downarrow} + 2\alpha/L, \downarrow}^\dagger, c_{k'_1, \downarrow}\} & \dots & \{c_{k_{N_\downarrow} + 2\alpha/L, \downarrow}^\dagger, c_{k'_{N_\downarrow}, \downarrow}\} \end{array} \right\|^2 \\ &= \frac{\sin^{2N_\downarrow} \alpha}{L^{2N_\downarrow}} \left\| \begin{array}{ccc} 1 & & 1 \\ \sin\left(\frac{k_1 - k'_1}{2} + \frac{\alpha}{L}\right) & \dots & \sin\left(\frac{k_1 - k'_{N_\downarrow}}{2} + \frac{\alpha}{L}\right) \\ \vdots & \ddots & \vdots \\ 1 & & 1 \\ \sin\left(\frac{k_{N_\downarrow} - k'_1}{2} + \frac{\alpha}{L}\right) & \dots & \sin\left(\frac{k_{N_\downarrow} - k'_{N_\downarrow}}{2} + \frac{\alpha}{L}\right) \end{array} \right\|^2. \end{aligned}$$

This determinant is actually a Cauchy determinant and can be expressed as a product, so we end up with

$$|\langle \tilde{f}_\downarrow | \hat{R} | \tilde{G}_\downarrow \rangle|^2 = \frac{\sin^{2N_\downarrow} \alpha}{L^{2N_\downarrow}} \frac{\prod_{j>i} \sin^2 \frac{k_j - k_i}{2} \prod_{j>i} \sin^2 \frac{k'_j - k'_i}{2}}{\prod_{j,i} \sin^2 \left(\frac{k'_i - k_j}{2} + \frac{\alpha}{L} \right)}. \quad (32)$$

For the special $\alpha=0$ [where $A'_\uparrow(\omega, k) = L \delta(\omega) \delta_{k,0}$] and $\alpha=\pi$ cases, taking the suitable limits, we recover the results of Eqs. (17) and (23), respectively. In the $\alpha=\pi$ case the phase shift equals $2\pi/L$, which is exactly the spacing between two adjacent k values, thus the orthogonality catastrophe is absent.

Following the same approach, for the photoemission part we get

$$B_\uparrow(k, \omega) = \frac{1}{L} \sum_{k' \in \text{FS}_\uparrow} B'_\uparrow(\omega - \varepsilon_\uparrow(k'), k - k') \quad (33)$$

with

$$\begin{aligned} B'_\uparrow(\omega, k) &= L \sum_f |\langle \tilde{f}_\downarrow | e^{-i a \hat{n}_{0,\downarrow}} \hat{R}^\dagger | \tilde{G}_\downarrow \rangle|^2 \delta(\omega - E_{\text{GS},\downarrow} \\ &\quad + E_{f,\downarrow}) \delta_{k, P_{\text{GS},\downarrow} - P_{f,\downarrow}}. \end{aligned} \quad (34)$$

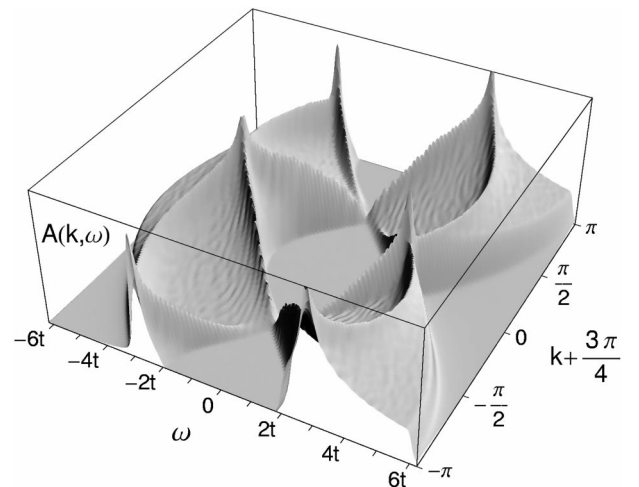


FIG. 3. The spectral function for $\alpha=3\pi/4$ and $n=1$. Here the Fermi energy is at $\omega=0$.

TABLE I. The exponents in the local spectral function [Eq. (15)].

α	0	$\pi/4$	$\pi/2$	$3\pi/4$	π
$2(\alpha/\pi)^2$	0	1/8	1/2	9/8	2
$2(\alpha/\pi-1)^2$	2	9/8	1/2	1/8	0

The product in Eq. (32) can be evaluated numerically and spectral functions for relatively large systems can be obtained. The numerical result for some large size systems is presented in Fig. 2. Starting from $\alpha=0$, we observe that there is an overall shift in momentum proportional to $-2\alpha n_{\downarrow}$ (which we compensated for in the figure), and that apart from the main contribution, which follows the cosine-like dispersion, additional continuumlike features appear. Finally, for even larger values of α another cosinelike feature appears with a considerable weight.

Alternatively, for the low-energy part, further analytical considerations can be applied.⁷ Starting from Eq. (32), the weights of the peaks can be expressed via Γ functions in the $L \rightarrow \infty$ limit, leading to the power-law behavior of the Tomonaga-Luttinger liquid spectral function (Fig. 3), and the exponents can be associated with the phase shift. We find singularities where the momenta of the final state are closely packed. These happen at

$$k_{\uparrow}^{(\nu)} = \nu \pi n_{\uparrow} - 2\alpha n_{\downarrow}, \quad (35)$$

with ν an odd integer. The most important ones for small α are those with $\nu = \pm 1$, which coincides with the Fermi momenta $k_{F,\uparrow}^{\pm}$. As we can follow in Fig. 2, by increasing α we get the weight for the tower at $k_{\uparrow}^{(3)}$, which eventually be-

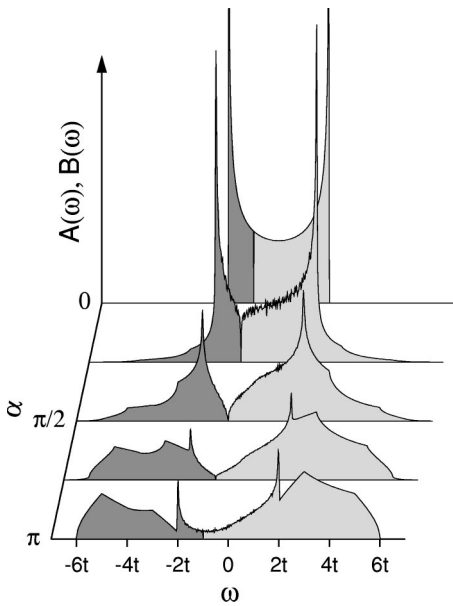


FIG. 4. The local spectral functions $B(\omega)$ (darker) and $A(\omega)$ (lighter shading) for $n=2/3$. α changes from 0 (noninteracting case, top curve) to π (bottom plot) in increments of $\pi/4$. To minimize finite-size effects, the curves show the average of $L=303, 279, 255, 231, 207$, and 183.

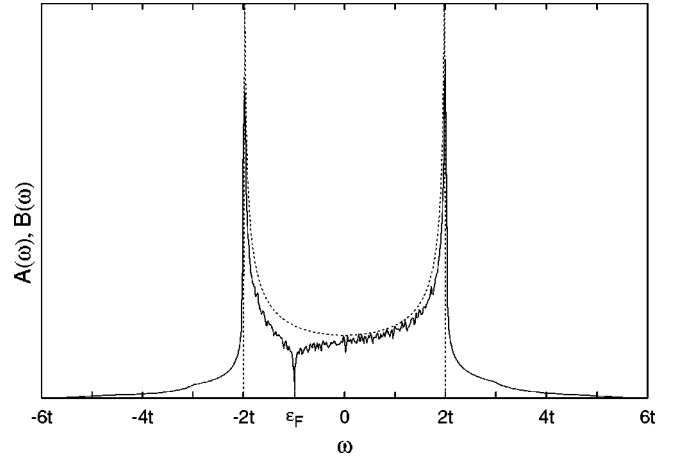


FIG. 5. To illustrate the weight transfer for small α , we compare the local spectral function for $\alpha=\pi/4$ (solid line) to the $\alpha=0$ case (dashed). The $\alpha=\pi/4$ case behaves as $A(\omega) \sim |\omega - \epsilon_F|^{1/8}$ near the Fermi energy.

comes symmetric with $k_{\uparrow}^{(1)}$ for $\alpha=\pi$, while the weight of the tower at $k_{\uparrow}^{(-1)}$ disappears at the same time. The primed spectral functions in Eq. (26) have a simple behavior near $k=0$,

$$A'_{\uparrow}(k, \omega) \propto [(\omega - \epsilon_F)^2 - u^2 k^2]^{(\alpha/\pi)^2 - 1}, \quad (36)$$

while near $k=2\pi n_{\downarrow}$,

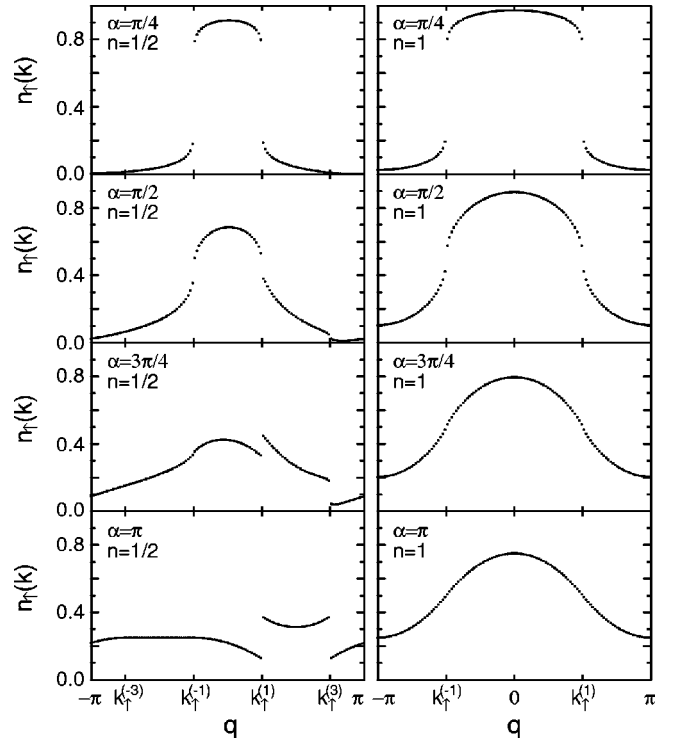


FIG. 6. The evolution of the momentum distribution function $n_{\uparrow}(k)$ as a function of α for $n=1/2$ (left) and $n=1$ (right plots) (as in Fig. 2). The shift of the Fermi momenta $k_{\uparrow}^{(\nu)}$ is compensated for by introducing $q = k + \alpha n$ in the plot.

$$A'_\uparrow(k, \omega) \propto [(\omega - \varepsilon_F)^2 - u^2(k - 2\pi n_\downarrow)^2]^{(\alpha/\pi - 1)^2 - 1}. \quad (37)$$

This leads to the power-law behavior of the $A_\uparrow(k, \omega)$ as presented in Eq. (14). The values of the exponents are tabulated for some selected α in Table I.

The weight transfer can be quantified by observing the sum rules. While the zeroth momentum is constant,

$$\int_{-\infty}^{\varepsilon_F} B_\uparrow(\omega) d\omega = n_\uparrow, \quad (38)$$

$$\int_{\varepsilon_F}^{+\infty} A_\uparrow(\omega) d\omega = 1 - n_\uparrow,$$

the first integral already shows the large weight transferred (Figs. 4 and 5) to energies far from the Fermi energy,

$$\begin{aligned} \int_{-\infty}^{\varepsilon_F} \omega B_\uparrow(\omega) d\omega &= \sum_i \langle G | c_{i,\uparrow}^\dagger [H, c_{i,\uparrow}] | G \rangle \\ &= -\frac{2t}{\pi} \sin(\pi n_\uparrow) \\ &\quad - \frac{4t}{\pi} n_\uparrow \sin(\pi n_\downarrow) (1 - \cos \alpha), \end{aligned}$$

$$\begin{aligned} \int_{\varepsilon_F}^{+\infty} \omega A_\uparrow(\omega) d\omega &= \sum_i \langle G | c_{i,\uparrow} [H, c_{i,\uparrow}^\dagger] | G \rangle \\ &= \frac{2t}{\pi} \sin(\pi n_\uparrow) + \frac{4t}{\pi} (1 - n_\uparrow) \\ &\quad \times \sin(\pi n_\downarrow) (1 - \cos \alpha). \end{aligned} \quad (39)$$

The weight transfer to higher energies is the largest for $\alpha = \pi$ and at half-filling.

Finally, in Fig. 6 we present the momentum distribution function $n_\uparrow(k)$. We can clearly observe the algebraic discontinuity at $k = k_\uparrow^{(\pm 1)}, k_\uparrow^{(3)}$ for $0 < \alpha < \pi$. For $\alpha = \pi$ (lower plots) there is a jump $\Delta n_\uparrow(k) = (1 - 2n_\downarrow)^2$ at $k = k_\uparrow^{(1)}$ and $k_\uparrow^{(3)}$ coming from the coherent part in the spectral function given by Eq. (23).

IV. CONCLUSIONS

We have presented the exact one-electron Green's function for a model Fermi system in 1D with a non-Fermi-liquid behavior for essentially any value of the interaction strength. The Green's function for this system obtained here does require some numerics and is not totally analytical. However, unlike the situation in projected models, such as the t - J model, it satisfies the sum rules familiar from text books for weakly interacting Fermi liquids (e.g., the complete electron sum rule with large ω behavior of G as $1/\omega$). This feature makes the present model particularly interesting in the context of the program of reconstruction of the spectral function from its moments (e.g., see Ref. 15).

ACKNOWLEDGMENTS

K.P. acknowledges the financial support of the Hungarian OTKA D32689 and Bolyai 118/99. We thank M. Randeria for interesting discussions.

¹I.E. Dzyaloshinsky and A.I. Larkin, Zh. Éksp. Teor. Fiz. **65**, 411 (1973) [Sov. Phys. JETP **38**, 202 (1974)].

²H. Shiba and M. Ogata, Int. J. Mod. Phys. B **5**, 31 (1991).

³S. Tomonaga, Prog. Theor. Phys. **5**, 349 (1950); J.M. Luttinger, J. Math. Phys. **4**, 1154 (1963); D.C. Mattis and E. Lieb, *ibid.* **6**, 304 (1965).

⁴F.D.M. Haldane, Phys. Rev. Lett. **45**, 1358 (1980); J. Phys. C **14**, 2585 (1981).

⁵J. Voit, Rep. Prog. Phys. **58**, 977 (1995).

⁶S. Sorella and A. Parola, J. Phys.: Condens. Matter **4**, 3589 (1992).

⁷K. Penc, K. Hallberg, F. Mila and H. Shiba, Phys. Rev. B **55**, 15 475 (1997); K. Penc, F. Mila, and H. Shiba, Phys. Rev. Lett. **75**, 894 (1995).

⁸M. Arikawa, Y. Saiga, and Y. Kuramoto, Phys. Rev. Lett. **86**, 3096 (2001).

⁹Y. Kato, Phys. Rev. Lett. **81**, 5402 (1998).

¹⁰H.J. Schulz and B.S. Shastry, Phys. Rev. Lett. **80**, 1924 (1998); **82**, 2410 (1999).

¹¹A.E. Borovik, A.A. Zvyagin, V. Yu. Popkov, and Yu. M. Strzheimchnyi, Pis'ma Zh. Eksp. Teor. Fiz. **55**, 293 (1992) [JETP Lett. **55**, 292 (1992)]; A.A. Zvyagin, Fiz. Nizk. Temp. **18**, 1029 (1992) [Sov. J. Low Temp. Phys. **18**, 723 (1992)]; Phys. Rev. Lett. **82**, 2409 (1999).

¹²A. Osterloh, L. Amico, and U. Eckern, Nucl. Phys. B **588**, 531 (2000).

¹³P.W. Anderson, Phys. Rev. Lett. **18**, 1049 (1967).

¹⁴A.A. Aligia, K. Hallberg, C.D. Batista, and G. Ortiz, Phys. Rev. B **61**, 7883 (2000), and references therein.

¹⁵M.R. Norman, H. Ding, H. Fretwell, M. Randeria, and J.C. Campuzano, Phys. Rev. B **60**, 7585 (1999); A. Paramekanti, M. Randeria, and N. Trivedi, Phys. Rev. Lett. **87**, 217002 (2001).